OpenPack: A Large-scale Dataset for Recognizing Packaging Works in IoT-enabled Logistic Environments

Naoya Yoshimura¹, Jaime Morales¹, Takuya Maekawa¹, Takahiro Hara¹

¹Osaka University 1-5 Yamadaoka, Suita, Osaka, Japan

Abstract

Unlike human daily activities, existing publicly available sensor datasets for work activity recognition in industrial domains are limited by difficulties in collecting realistic data as close collaboration with industrial sites is required. This also limits research on and development of AI methods for industrial applications. To address these challenges and contribute to research on machine recognition of work activities in industrial domains, in this study, we introduce a new large-scale dataset for packaging work recognition called OpenPack. OpenPack contains 53.8 hours of multimodal sensor data, including keypoints, depth images, acceleration data, and readings from IoT-enabled devices (e.g., handheld barcode scanners used in work procedures), collected from 16 distinct subjects with different levels of packaging work experience. On the basis of this dataset, we propose a neural network model designed to recognize work activities, which efficiently fuses sensor data and readings from IoT-enabled devices by processing them within different streams in a ladder-shaped architecture, and the experiment showed the effectiveness of the architecture. We believe that OpenPack will contribute to the community of action/activity recognition with sensors. Open-Pack dataset is available at https://open-pack.github.io/.

1 Introduction

In industrial environments such as factories and logistics centers, human workers continue to perform important roles in ensuring flexible responses to rapidly changing demands of customers and suppliers. Specifically, the number of workers employed in logistics continues to increase (Michel 2016; Schlögl and Zsifkovits 2016), and this trend is expected to persist in the future (Klumpp et al. 2019; Reining et al. 2019; Yavas and Ozkan-Ozen 2020). For example, Amazon ships 2.5 billion packages annually in the U.S., which highlights the significance of streamlining shipping processes in global and regional supply chains. Aiming to streamline work processes performed by human workers and enable enterprises to make business decisions based on granular work information, digitization is being widely implemented in industrial environments as part of the Industry 4.0 transformation. In Industry 4.0, digitized data on human motion acquired from sensor systems and readings from IoT-enabled devices (e.g., connected handheld terminals) are expected to be used to achieve work activity recognition to quantify and streamline work processes performed

by human workers. Therefore, activity recognition for human workers in industrial domains has recently attracted attention as a topic of active research (Xia et al. 2019, 2020; Morales et al. 2022; Yoshimura et al. 2022).

However, the following challenges should be addressed to enhance work activity recognition studies.

- Lack of datasets for industrial domains: The amount of publicly available datasets for industrial domains containing complex activities (e.g., manufacturing and packing/picking tasks) remains limited, and many of the available activity recognition datasets focus only on simple daily activities (e.g., walking and running). Fig. 1 shows a typical series of packaging tasks iterated several times, with each iteration of the process (i.e., period) comprising a sequence of operations in which the acceleration data indicate the complexity of operations. While a dataset is available for the logistics domain (Niemann et al. 2020), the activity classes used do not reflect the complex work process¹. In addition, the size of many existing datasets does not suffice to fulfill the basic requirements of deep learning.
- Limited modality: Many public datasets for manual tasks provide only vision-related modalities. However, because many types of manufacturing equipment and storage systems are installed in industrial environments, occlusion tends to pose challenges in applying visiononly approaches.
- Difficulties in human–IoT data coordination: Although digitization is progressing in actual industrial domains as part of the development of Industry 4.0, to the best of our knowledge, no datasets on activity recognition that include both sensory data on human motions and readings from IoT-enabled devices operated by the human workers are publicly available.
- Lack of rich metadata: Many of the available datasets

¹The LARa dataset (Niemann et al. 2020) does not consider the difference between work activities (e.g., packing items and making a shipping box) in the definition of activity classes. Instead, these activities are defined as handling-related classes, including handling (upward), handling (centered), and handling (downward), which are defined as handling items and boxes at different positions. For example, in handling (upward), a subject handles items with at least one hand reaching shoulder height.

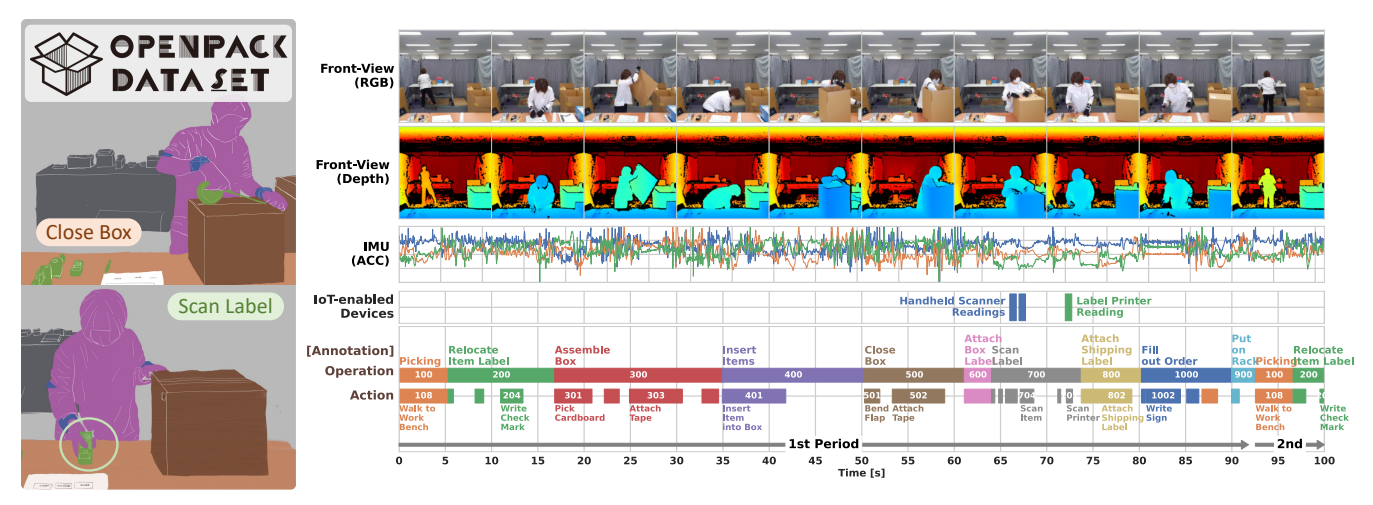


Figure 1: Illustration of the OpenPack dataset. A subject iterated a typical series of packaging works, with each iteration of the process (i.e., period) comprising a sequence of complex operations.

do not provide a rich set of metadata related to manual works such as a set of the items to be packed, which limits the understanding of recognition results and the design of new, enhanced research tasks.

To address these challenges, in this study, we propose a new multimodal dataset for packaging work recognition in logistics, called OpenPack (Fig. 1). OpenPack consists of 20, 129 instances of activities (operations) and 52, 529 instances of actions with 9 types of modalities captured from 16 distinct subjects with various levels of experience performing packaging tasks. The features of Open-Pack are summarized as follows. (i) OpenPack is the first large-scale dataset for packaging work recognition that contains readings from IoT-enabled devices. (ii) OpenPack provides multimodal work activity data, including sensory data from body-worn inertial measurement units (IMUs), depth images, and LiDAR point clouds for use in research on multi-/crossmodal, IMU-only, and vision-only work activity recognition according to conditions in an expected target environment. (iii) OpenPack also provides a rich set of metadata such as subjects' levels of experience in packaging work as well as their physical characteristics, enabling the design of various research tasks (e.g., assessment of workers' performance) in addition to basic work activity recognition.

One of the main features of OpenPack is that it contains readings from IoT-enabled devices operated by subjects. Although high performance is required of work activity recognition methods in industrial domains to develop critical applications such as outlier detection, even state-of-the-art activity recognition methods cannot achieve sufficient performance by using noisy sensor data (e.g., vision-based and IMU sensor data). Leveraging high-confidence readings from IoT-enabled devices, which strongly relate to activities performed (e.g., readings from a handheld scanner to detect the "scan label" operation), is expected to provide a key enabler to achieve precise recognition for real applications.

Although readings from IoT-enabled devices are highly

confident, they are sparse in time because in general they are recorded only when a worker operates a device. Therefore, an efficient strategy of activity recognition using such IoT data with noisy sensor data (e.g., IMU data) may consider (i) leveraging available readings from IoT-enabled devices as high-confidence anchors and then (ii) predicting an activity class at a time step when readings are unavailable by referring to the sensor data and anchors surrounding the time step of interest. That is, because activity classes can be precisely predicted at a time step when readings from IoT-enabled devices are available, we predict an activity class at a time step when IoT data are unavailable by referring to surrounding IoT data as anchors. However, even for state-of-the-art human activity recognition methods that assume sensor data as input, there is no guarantee that a recognition model trained by these methods would learn the abovementioned efficient recognition strategy if sensor and IoT data were simply fed into the recognition model. Therefore, in this paper, we propose a novel activity recognition model for sensor and IoT data, called a ladder-shaped two-stream network (LTS-Net), which is designed to be guided to learn the abovementioned strategy. LTS-Net processes sensor data and high-confidence IoT data in different streams and updates information in each stream by referring to information in different streams while preserving information on the IoT data in deeper layers.

The key contributions of this research are summarized as follows: i) To the best of our knowledge, OpenPack is the largest dataset on industrial work activity recognition. We expect this data to contribute to research on industrial AI systems by providing a challenging task, that is, to complex activity recognition via sensor and sparse IoT data. ii) We propose LTS-Net to effectively utilize sparse readings from IoT devices via a ladder structure. iii) The results of the experimental evaluation showed that LTS-Net significantly improved the performance, indicating the usefulness of the readings from IoT devices and the effectiveness of the ladder structure in our method.

Table 1: Overview of public datasets of human activities/works. D: Depth, Acc: Acceleration data, Gyro: Gyroscopic data, Ori: Orientation sensor data, EDA: Electrodermal activity, BVP: Blood volume pulse, Temp: Temperature.

Domain	Datasets	Type of Task	Recording Length	Activity Class*	# of work period	Annotated Instances	Subjects	Modality	IoT Devices	View	Year
	MHAD	Daily Actions	82m	11	N/A	660	12	RGB+D+Keypoints+Acc+Mic	No	12	2013
Multi-modal	UTD-MHAD	Daily Actions	9m	27	N/A	180	8	RGB+D+Keypoints+Acc+Gyro	No	1	2015
	MMAct	Daily Actions	17h35m	37	N/A	36,764	20	RGB+D+Keypoints+Acc+Gyro +Ori+WiFi+Pressure	No	4+Ego	2019
Cooking	CMU-MMAC	Cooking	-	5	186	186	39	RGB+D+Keypoints+Acc+Mic	Yes (RFID)	5	2010
Cooking	50 Salads	Cooking	4h	52	50	2,967	25	RGB+D+Acc	Yes (Acc)	1	2013
	COIN	Instruction Video	476h38m	180	N/A	46,354	N/A	RGB (Youtube)	No	N/A	2019
Procedural Activity	IKEA-ASM	Furniture Assembly	35h16m	33	371	16,764	48	RGB+D+Keypoints	No	3	2021
	Assembly101	Toy Assembly	42h+	202	362	1M+	53	RGB	No	12	2022
	InHARD	Industrial Actions	18h30m	14 + 72	38	4800	16	RGB+Keypoints (3D)	No	3	2020
	ABC Bento	Bento Packaging	3h22m	10	199	151	4	MOCAP	No	1	2021
Industrial	LARa	Picking	- 14h50m	8 + 19	324	8878	16	RGB+Keypoints (3D) +Acc+Mic	No	1	2020
	LAKa	Packaging	141130111	0 + 17	125	2103	10		NO	1	+2022
	OpenPack	Packaging	53h50m	10 + 32	2048	20, 129	16	D+Keypoints+LiDAR+Acc+Gyro +Ori+EDA+BVP+Temp	Yes	2	2022

*When action classes are defined in a hierarchical manner, the numbers of classes in different levels are shown with separator "+". In the case of OpenPack, they correspond to # of operations and actions.

2 Related Work

2.1 Datasets on Manual Tasks

Although many multimodal, vision-based, and IMU-based datasets for daily activity recognition have been made publicly available (Spriggs, De La Torre, and Hebert 2009; Ofli et al. 2013; Chen, Jafari, and Kehtarnavaz 2015; Kong et al. 2019), the number of publicly available datasets for work activity recognition in industrial domains remains limited. Table 1 summarizes the attributes of datasets on human activities and manual labor. To the best of our knowledge, the LARa dataset (Niemann et al. 2020, 2022) is the only dataset on work activity recognition in logistics. However, the activity classes used in the dataset do not reflect the complexity of work processes well, and the number of activity (operation) instances is limited, as mentioned in the introduction. In addition, the dataset does not provide readings from IoTenabled devices or a rich set of metadata.

The InHARD dataset (Dallel et al. 2020) and the ABC Bento packaging dataset (Alia et al. 2021) are designed to accelerate human-robot collaboration in industrial settings. The InHARD dataset consists of RGB and 3D keypoint data from 16 subjects collected while they were assembling various parts and components. The ABC Bento Packaging dataset is a dataset that captures activities related to bento packaging. This dataset focuses on common mistakes made by bento manufacturers, such as "forgetting to put in ingredients," and provides labels only for outlier types. The ABC Bento Packaging dataset is quite small to be applied to data-driven algorithms, such as deep learning. These visionbased datasets also lack sensor data modalities. In contrast, OpenPack is a large-scale dataset containing 20, 129 work operation instances with multimodal sensor data. The activity label set used in this dataset was designed based on operations specified in instruction documents used at actual logistic centers. In addition, OpenPack provides a rich set of metadata such as the size and item code (JAN code) of each item and a set of items to be packed.

Datasets of various complex procedural activities are also available. Specifically, many multimodal/vision-based cooking activity datasets are available such as CMU-MMAC (Spriggs, De La Torre, and Hebert 2009), 50 Sal-

ads dataset (Stein and McKenna 2013), Breakfast Actions Dataset (Kuehne, Arslan, and Serre 2014), EPIC-KITCHENS (Damen et al. 2018), and the Cooking Activity Dataset (Lago et al. 2020). Vision-based datasets focused on procedural activities other than cooking include IKAE-ASM (Ben-Shabat et al. 2021) and Assembly101 (Sener et al. 2022) for assembling furniture and toys, and COIN, a collection of instructional videos collected from YouTube. As noted above, many multimodal or vision-based datasets on manual tasks in daily life have been made publicly available. In contrast, the availability of public datasets for industrial domains remains limited, and OpenPack is the first large-scale dataset for activity recognition in industrial domains. This may be attributed to the difficulties in collecting datasets for industrial domains compared to everyday tasks. Collecting data for industrial applications requires close collaboration with industrial engineers working in an actual target environment to coordinate an experimental environment with various equipment for the target task, to define a set of activity labels by obtaining an actual work instruction document used in the target industrial environment, and to employ workers with experience in the target task as research subjects.

2.2 Sensor-Based Activity Recognition Methods

A number of activity recognition methods have been proposed. Methods that use IMU sensors include DeepConvL-STM (Singh et al. 2020), U-Net (Zhang et al. 2019), and Conformer (Kim et al. 2022). LOS-Net (Yoshimura et al. 2022) and MGA-Net (Morales et al. 2022) were designed to recognize activities in industrial applications. Vision-based approaches have also been proposed, such as I3C (Carreira and Zisserman 2017), ST-GCN (Yan, Xiong, and Lin 2018), and MVT (Yan et al. 2022). Although vision-based methods are very powerful, packaging work is typically subject to occlusion caused by large items or boxes. Therefore, we evaluated the proposed method on IMU sensor data. Several sensor fusion methods have been proposed for multimodal activity recognition, such as Multi-GAT (Islam and Iqbal 2021), and early/late fusion (Münzner et al. 2017). Data from IoT-devices are sparse but have a strong relation-

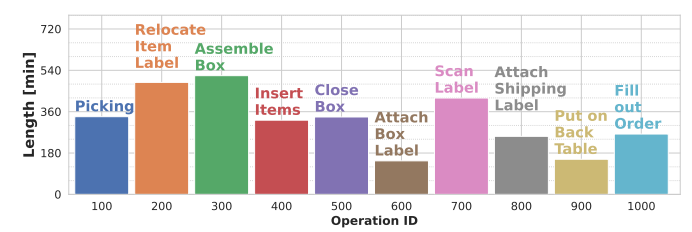


Figure 2: Total recording length of each operation

ship with specific activity classes, which is quite different from other sensor data. However, these methods do not consider this property.

3 OpenPack Dataset

OpenPack² is the first multimodal large-scale dataset for activity recognition in industrial domains. 16 distinct participants packed 3,956 items in 2,048 shipping boxes in total, and the total duration of our dataset is 53.8 hours, consisting of 104 sessions (see below). The total number of collected work operations and actions are 20,129 and 52,529 respectively³. The average lengths of operations and actions are 9.2 and 4.1 seconds respectively. OpenPack is the largest industrial dataset that includes both vision and wearable sensor data with precise labels by annotators. The most similar dataset to OpenPack is LARa (Niemann et al. 2020), but the total data duration of LARa is 14.8 h. Further details are introduced as follows.

3.1 Packaging Work

As shown in Fig. 1, a typical series of complex operations is iterated, with each iteration (i.e., period) comprising a sequence of operations such as assembling a shipping box and filling the box with items. In a given work period, a worker processes a single shipping order. That is, the worker picks items in a specified order, double-checks the items, assembles a shipping box, fills the box with the items, and so forth to complete the order. When performing specific operations, the worker uses IoT-enabled devices such as a handheld barcode scanner, and the operation is recorded and transmitted by the device. Because the size of items to be packed, the number of items, and the size of shipping items depend on shipping orders, sensor data collected in different work periods and the duration of the same operation in different work periods vary. The task of recognizing specific actions is challenging owing to these characteristics of packaging work.

3.2 Data Construction

Classes Operation classes used in OpenPack were defined based on an instruction document used in an actual logistics center. The document specifies a sequence of operations performed by a worker, and each worker in the center performs operations according to the document. Therefore, the basic activities performed by all workers, i.e., operations, were

used to label the dataset. Our dataset contains ten classes of operations, including picking, relocating item labels, assembling boxes, inserting items, closing the box, attaching a label to the box, scanning the label, attaching a shipping label, placing the item on a rack, and filling out an order. Note that many other logistics centers also utilize patterns of operations very similar to those used in this study. Fig. 2 shows the distribution of the total recording length of each operation.

An instructional document also contains a description of each operation that explains how to perform the operation. For example, a description of the "relocate item label" operation is given as "Remove the label from the items and place it on the bottom margin of the packaging list. Check the product name and quantity on the list and label with a ballpoint pen." Based on the description, we also defined a set of action classes included in each operation. For example, as shown in Fig. 1, the "assemble box" operation is composed of four actions, including "pick up cardboard," "bend flap," "attach tape," and "turn over box." Our dataset contains 32 action classes in total. The action classes are useful to enable a manager in a logistics center to assess the status of a job in progress in detail.

Subjects We invited 16 subjects to participate in our data collection process. The ages of the subjects were ranged from 20 and 50. 12 subjects had experience in packaging work ranging from 1 month to 4 years. In addition, 4 subjects did not have work experience. One subject was left-handed. Each subject was assigned a consistent identifier throughout the entire dataset. The supplementary information included the detailed information about the subjects.

Sessions and Work Periods In our dataset, a session is composed of iterations of work periods. In each work period, a subject processes the items on an order sheet. To complete the order, the subject performs the operations specified in the instruction document.

3.3 Data Collection

Collection Environment We collected data in a dedicated environment shown in Fig. 3. With the help of industrial engineers, we constructed a 3m × 5m environment designed to simulate an actual workspace in a logistics center. The environment mainly comprised a workbench, a back table on which items were placed after being picked from shelves by another worker, boxes containing air cushions, and a trash can. The distance between the workbench and the back table was approximately 2 meters, and a worker worked between the bench and the back table. A handheld barcode scanner, a printer, and craft tapes used for packaging were located on the right side of the table. Four types of cardboard boxes were available for packing, including small, medium, large, and extra-large sizes, as shown in Fig. 3.

Data Modalities OpenPack provides nine data modalities, including acceleration, gyroscope, quaternion, blood volume pulse (BVP), and electrodermal activity (EDA) data, temperature, as well as keypoints, a LiDAR point cloud, and depth images collected in the dedicated environment. Four

²https://open-pack.github.io/

³These statistics were obtained on the OpenPack dataset (v0.3.1).

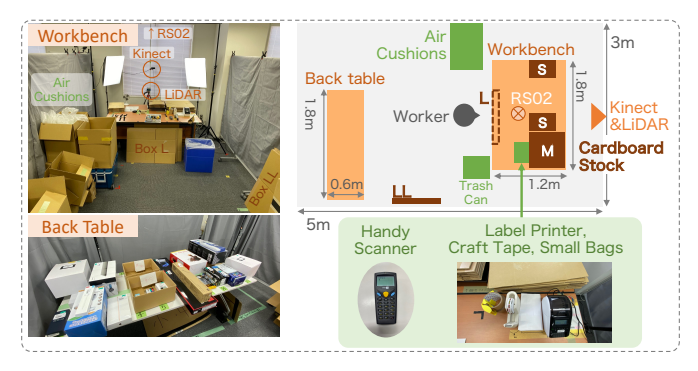


Figure 3: Environmental setup

IMU units were attached to the subject's left and right wrists and upper arms to collect acceleration data on three axes, as well as gyroscope and quaternion data at 30 Hz. In addition, two Empatica E4 sensors were attached to the subject's left and right wrists to collect BVP and EDA signals at 64 Hz and 4 Hz, respectively, in addition to acceleration data at 32 Hz. Kinect and LiDAR sensors were installed as front-view cameras and RealSense (RS02) as a top-view camera as shown in Fig. 3. The LiDAR sensor was considered effective in accurately tracking the subject's position when they were away from the workbench.

OpenPack also provides operational logs of IoT-enabled devices, i.e., the handheld scanner and label printer, in the environment. The operational logs of the handheld scanner, for example, contain a time-stamp of a scan and an identifier of a scanned item. These are highly reliable sources of information for recognizing the scanning operation and may improve recognition performance. The specifications of the sensors and an overview of the data are provided in the supplementary information.

Data Collection Procedure Before data collection, each subject received instructions related to the outline of the experiment and the operations to be performed based on the instruction document. Subsequently, we obtained the informed consent of the subjects, who then practiced the packaging work by performing work periods up to five times. Subsequently, we activated and calibrated the sensors and attached the wearable sensors to the subjects.

The subjects iterated up to five data collection sessions within 6 h (including a 60-min lunch break). At the beginning of each session, the subject received 20 order sheets and then sequentially processed the sheets. That is, the subject completed 20 shipping boxes in the session. A 15-min break was included between two consecutive sessions. Note that each session was conducted under either one of the following four scenarios. After data collection, the data were labeled by annotators with 5-6 years of experience in human/animal activity data labeling by reference to the RGB images with the help of industrial engineers.

Scenarios The difficulties in packaging work recognition depend on various factors in logistics centers. For example, (i) some experienced workers alter operational procedures to improve efficiency, (ii) the size and the number of items

greatly affect workers' movements and sensor data, and (iii) workers sometimes perform irregular activities. To simulate these situations and factors, we prepared the following four scenarios. Scenario 1 was the most basic setup, in which workers followed instructions in principle. Scenario 2 allowed workers to make changes to the work procedures according to their own judgment and involved a richer variety of combinations by adding new items. Scenario 3 introduced irregular activities, such as picking items for several boxes at once. In Scenario 4, a sound alarm was introduced to hurry workers to simulate a busy situation. For more details about each scenario, refer to the supplementary information.

Metadata OpenPack provides a rich set of metadata, which is mainly composed of subject- and order-related metadata. The subject-related metadata contains information regarding each of the participants' experience in packaging tasks, as well as their dominant hand, gender, and age.

Order-related metadata contains information regarding an order sheet processed by a subject in a work period. Open-Pack assumes an online order management system and provides information regarding an identifier of an order and a set of items to pack in the order. The management system also stores information regarding an identifier, product code, and the size of each item. These identifiers are used to manage items in an order management system. In contrast, product codes are unique numbers for each item, which are widely used in retail sales and enable information to be retrieved regarding an item, such as product name, product type, and price. OpenPack also provides this information.

In addition to the above order information, which can be automatically obtained from the order management system, OpenPack also provides manually annotated metadata regarding mistakes and accidents in each period. For example, operations that a subject forgot to perform and those that were conducted in the wrong order were recorded.

Potential Research Tasks In addition to basic operation and action recognition using depth or wearable sensors, OpenPack enables various designs of research tasks, which includes the following: (i) transfer learning across workers/sensor positions, (ii) crossmodal transfer learning using, e.g., knowledge distillation (Kong et al. 2019), (iii) skill assessment using sensor data and metadata related to work experience as ground truth, (iv) failure detection using sensor data and metadata related to mistakes as ground truth, (v) counting the number of necessary actions or the number of packed items using sensor data, (vi) estimating workers' levels of fatigue using sensor and physiological data.

4 Ladder-Shaped Two-Stream Network with Sparse Anchoring (LTS-Net)

Based on the OpenPack dataset, we propose a new activity recognition model that effectively utilizes sparse readings from IoT-enabled devices. There is a strong connection between devices in use and a user's current activity. For example, when a subject uses a handheld scanner, the activity label for that moment would be "scan label." In this study, we leverage the high-confidence source, i.e., readings from

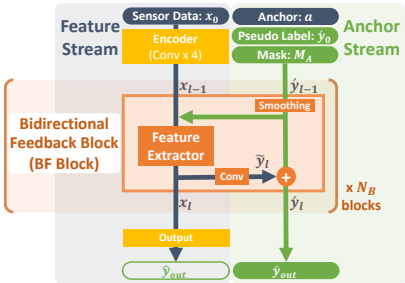


Figure 4: Architecture of Ladder-shaped Two-stream Network

IoT-enabled devices, as an anchor to precisely recognize activities (operations). To efficiently leverage anchors, we propose a LTS-Net for time-series classification (Fig. 4). The ladder-shape is composed of bidirectional feedback blocks (BF blocks) comprising two vertical streams, i.e., a feature stream and an anchor stream, and feedback branches that are used to exchange information between the streams. Sensor data (e.g., IMU data) are fed into the feature stream after initial feature extraction by the encoder, and feature extraction is performed. Anchors and pseudo-estimates of activity classes generated from the anchors are fed into the anchor stream, and the pseudo-estimates are refined in deeper layers. By performing feature extraction and activity class estimation in different streams, we can refine pseudo-estimates generated from high-confidence anchors by referring to sensor data while retaining the high-confidence information in deeper layers.

4.1 Preliminary

We assume that x_0 is time-series sensor data, such as acceleration and skeleton data, and $a \in \mathbb{R}^{N_A \times T}$ is derived from readings from IoT devices, i.e., anchors. The outputs of the model $\mathbf{\acute{y}}_{out} \in \mathbb{R}^{N_C \times T}$ are the probability of each activity (operation) label for each time step. N_A , N_C , and T denote the number of anchor channels, the number of activity classes, and the length of the time series, respectively. For example, when two types of usages of IoT-enabled devices are available, e.g., scanning with a handheld scanner and printing with a label printer, N_A is 2. When the handheld scanner (i-th channel) is used at time t, $a^{i,t}$ is set to 1. Otherwise, it is set to 0. In the example of the upper portion of Fig. 5, the use of the handheld scanner corresponds to the 1st channel and its corresponding value is 1 when it is used.

4.2 Anchor Stream

To efficiently leverage anchors, an anchor sequence a, a pseudo-label sequence $\mathbf{\acute{y}}_0$ generated from a, and an anchor mask M_A are fed into the anchor stream; Fig. 5 shows an example. $\mathbf{\acute{y}}_0 \in \mathbb{R}^{N_C \times T}$ is an initial pseudo-estimate of class probabilities calculated from a set of possible activity classes at each time step t determined based on the anchor. We define a function that calculates the possible activity set at time t as C(a,t). For example, when the handheld scanner is used at time t, i.e., $a^t = [1,0]^T$, $C(a,t) = \{\text{ScanLabel}\}$, which is determined based on labeled training data. In contrast, when no IoT devices are used at time t, i.e., $a^t = [1,0]^T$, $a^t = [1$

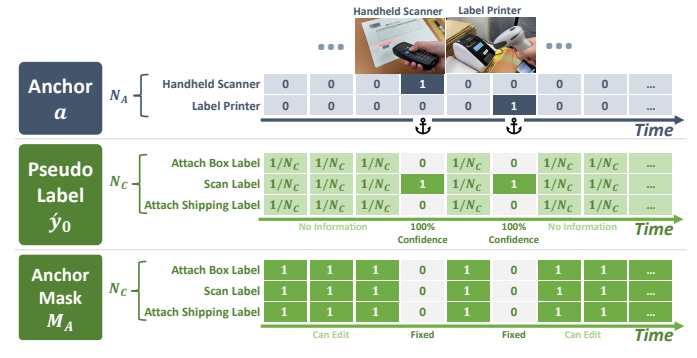


Figure 5: Examples of anchor, pseudo label, and anchor mask

 $[0,0]^{\mathrm{T}}$, $C(\boldsymbol{a},t)$ is a set of all the activity classes because we cannot determine specific possible activity classes based on \boldsymbol{a}^t . Refer to the supplementary information for the exact definition of $C(\boldsymbol{a},t)$. An initial estimate (pseudo-label) at time t for the c-th class is calculated as follows.

$$\label{eq:y0_ct} \dot{y}_0^{c,t} = \begin{cases} 1/|C(\boldsymbol{a},t)|, & c \in C(\boldsymbol{a},t) \\ 0, & otherwise \end{cases}$$

As shown in the middle panel of Fig. 5, when the handheld scanner was used, the element corresponding to Scan Label was 1, and the other elements were 0. When no IoT devices were used at time t, $|C(\boldsymbol{a},t)|$ was identical to N_C and the class probability (pseudo-label) was uniform, i.e., $1/N_C$, among all the classes. $\hat{\boldsymbol{y}}_0$ is updated within the deeper layers in the anchor stream by referring to sensor data features.

Avoiding changing the high-confidence parts in the pseudo-labels is important in deeper layers. An anchor mask $M_A \in \mathbb{R}^{N_C \times T}$ is introduced to specify elements of $\mathbf{\acute{y}}_l$ to be updated in the BF block. An element of the mask for the c-th class at time t, i.e., $M_A^{c,t}$, is defined as follows.

$$M_A^{c,t} = \begin{cases} 0, & \acute{y}_0^{c,t} \in \{0,1\} \\ 1, & otherwise. \end{cases}$$

As shown in the lower panel of Fig. 5, when probability 0 or 1 is assigned to the $\mathbf{y}_0^{c,t}$, the corresponding element of the mask is set to 0 because we want to fix the high-confident estimate. Otherwise, we assign 1 to allow updating the low-confident estimate in the BF block.

4.3 Bidirectional Feedback Block (BF Block)

As shown in Fig. 4, LTS-Net comprises multiple BF blocks, each of which consists of a pair of feedback branches and a set of modules between them. BF blocks extract features from sensor data and update $\mathbf{\acute{y}}_0$ to make predictions by referring to the extracted features. The inputs to the l-th block are the outputs of the previous block: $\mathbf{\emph{x}}_{l-1}$, $\mathbf{\emph{y}}_{l-1}$, and M_A . The output of this block is $\mathbf{\emph{x}}_l$ and $\mathbf{\emph{y}}_{l-1}$, with the same shape as the corresponding input.

Smoothing is first applied to the input pseudo-labels \hat{y}_{l-1} . This removes spontaneous activity transitions in the pseudo-labels and propagates the anchor information to the surroundings. The feature extractor is an arbitrary module that extracts features from sensor data. For example, convolutional layers, Conformer (Kim et al. 2022), a WPCP module

Table 2: F1-measures of methods

Tuest 2. I I measures of methods										
F1-measure		Macro	Weighted Avg.							
User	U0104	U0108	U0110	All	All					
DCL-SA	0.762	0.782	0.643	0.752	0.766					
DCL-SA (Early)	0.810	0.815	0.630	0.760	0.780					
DCL-SA (Late)	0.820	0.807	0.725	0.797	0.813					
Conformer	0.801	0.724	0.676	0.748	0.752					
Conformer (Early)	0.834	0.778	0.716	0.787	0.797					
LOS-Net	0.790	0.793	0.611	0.755	0.762					
LOS-Net (Early)	0.819	0.815	0.675	0.784	0.802					
LOS-Net (Late)	0.816	0.813	0.644	0.777	0.787					
LTS-Net (WPCP)	0.847	0.842	0.757	0.830	0.846					

(Yoshimura et al. 2022), etc. can be used. We also use $\hat{\mathbf{y}}_{l-1}$ and \boldsymbol{a} as additional inputs of the feature extractor to employ anchor information in the feature extraction. The output of the feature extractor \boldsymbol{x}_l is transformed to the same shape as $\hat{\mathbf{y}}_{l-1}$ by a 1D convolution and sigmoid function to output $\tilde{\mathbf{y}}_l \in \mathbb{R}^{N_C \times T}$, which is an estimate based mainly on sensor data. Then, $\hat{\mathbf{y}}_{l-1}$ is updated by using $\tilde{\mathbf{y}}_l$ as follows.

$$\mathbf{\acute{y}}_{l} = (1 - \beta M_{A})\mathbf{\acute{y}}_{l-1} + \beta M_{A}\mathbf{\~{y}}_{l}.$$

With this operation, the pseudo-label sequence is modified in each block while preserving anchor information. β controls the amount of update within a single block.

 \hat{y}_l from the last BF block is the final output of LTS-Net.

4.4 Training

The loss function of LTS-Net is calculated based on the soft-max cross-entropy $CE(\cdot)$ computed on the output of the anchor stream \hat{y}_{out} and the feature stream \hat{y}_{out} as follows:

$$\mathcal{L} = CE(\mathbf{gt}, \hat{\mathbf{y}}_{out}) + \gamma CE(\mathbf{gt}, \hat{\mathbf{y}}_{out}),$$

where gt denotes the ground truth and γ is a hyperparameter that controls the impact of \hat{y}_{out} . Adam optimizer with the cosine annealing learning rate scheduler (Loshchilov and Hutter 2016) is used for training. See the supplementary information for the detailed parameters of the method.

5 Evaluation

5.1 Evaluation Methodology

We evaluated LTS-Net on the OpenPack dataset. The data collected in Scenario 1 were used for evaluation, and operation recognition (semantic segmentation) was performed. Acceleration data from an IMU attached to the left wrist were used as the sensor data. Subjects U0104, U0108, and U0110 were used as test subjects and the remaining subjects were used as training subjects. The performance of our model was evaluated in terms of F1-measure. Because the ground truth was provided at 1 Hz, the outputs of the model were downsampled to 1 Hz before computing the metrics. We compared our LTS-Net to DeepConvLSTM + Self-Attention (DCL-SA) (Singh et al. 2020), Conformer (Kim et al. 2022), and LOS-Net (Yoshimura et al. 2022), which use only acceleration data as inputs. We also prepared early/late fusion models for each method, which also use IoT data. As a feature extractor of the LTS-Net, we used WPCP module and the number of BF block was set to 8.

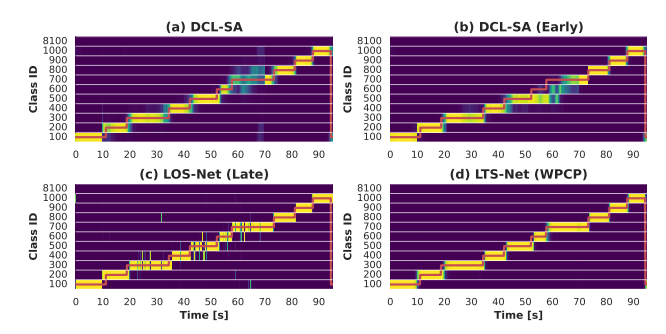


Figure 6: Examples of time-series data of ground truth (red line) and class estimates, i.e., probabilities. High- and low-class probabilities are yellow and blue, respectively.

The model parameters described in the original papers were used directly, whereas the optimization parameters, such as the learning rate, were tuned (see supplementary information).

5.2 Results

Table 2 shows the recognition performance on the test set of the models trained by changing the random seed 5 times. The F1-measure (macro avg) is approximately 0.75 for all the existing methods when data from IoT-enabled devices are unavailable. By adding data from IoT-enabled devices, the F1-measures of DCL-SA, Conformer, and LOS-Net improved by up to 0.04. The F1-measre of DCL-SA (Late), which is the best score among the existing methods, was 0.797 when data from IoT-enabled devices were used. The proposed LTS-Net (WPCP) method, which employs the WPCP module as the feature extractor, significantly outperformed DCL-SA (Late) in terms of F1-measure by 0.033 (p = 0.019 by Welch's t-test) and achieved 0.830 by effectively leveraging anchors. In particular, only LTS-Net achieved a score higher than 0.75 for U0110, whose skill level was Expert and work speed is much higher than the other training subjects. The same trend can be observed for the F1-measure (weighted average).

Figure 6 shows examples of model estimates. DCL-SA, which does not use anchors, failed to recognize the latter half of the scan label operation (Class ID: 700). Although DCL-SA (Ealry) and LOS-Net (Late) employed anchors related to a hand scanner, the estimates of the scan-label operation and surrounding operations were unstable compared with those of LTS-Net, indicating the ability of LTS-Net to efficiently fuse IoT and sensor data.

6 Conclusion

This study presented a new large-scale dataset for packaging work recognition called OpenPack. OpenPack contains 53.8 hours of multimodal sensor data, including depth images, IMU data, and readings from IoT-enabled devices. This dataset enables researchers to explore more challenging activity recognition methods for industries, such as collaboration with IoT devices. Furthermore, we propose LTS-Net to effectively utilize sparse readings from IoT devices. The evaluation results on our dataset have demonstrated the effectiveness of the proposed two-stream architecture.

References

- Alia, S. S.; Adachi, K.; Nahid, N.; Kaneko, H.; Lago, P.; and Inoue, S. 2021. Bento Packaging Activity Recognition Challenge.
- Ben-Shabat, Y.; Yu, X.; Saleh, F.; Campbell, D.; Rodriguez-Opazo, C.; Li, H.; and Gould, S. 2021. The ikea asm dataset: Understanding people assembling furniture through actions, objects and pose. In <u>Proceedings of the IEEE/CVF Winter Conference on Applications of Computer Vision</u>, 847–859.
- Carreira, J.; and Zisserman, A. 2017. Quo vadis, action recognition? a new model and the kinetics dataset. In Proceedings of the IEEE Conference on Computer Vision and Pattern Recognition, 6299–6308.
- Chen, C.; Jafari, R.; and Kehtarnavaz, N. 2015. UTD-MHAD: A multimodal dataset for human action recognition utilizing a depth camera and a wearable inertial sensor. In Proceedings of the IEEE International Conference on Image Processing, 168–172. IEEE.
- Dallel, M.; Havard, V.; Baudry, D.; and Savatier, X. 2020. InHARD-Industrial Human Action Recognition Dataset in the Context of Industrial Collaborative Robotics. In Proceedings of the IEEE International Conference on Human-Machine Systems, 1–6. IEEE.
- Damen, D.; Doughty, H.; Farinella, G. M.; Fidler, S.; Furnari, A.; Kazakos, E.; Moltisanti, D.; Munro, J.; Perrett, T.; Price, W.; and Wray, M. 2018. Scaling Egocentric Vision: The EPIC-KITCHENS Dataset. In <u>Proceedings of the European Conference on Computer Vision</u>.
- Islam, M. M.; and Iqbal, T. 2021. Multi-gat: A graphical attention-based hierarchical multimodal representation learning approach for human activity recognition. <u>IEEE</u> Robotics and Automation Letters, 6(2): 1729–1736.
- Kim, Y.-W.; Cho, W.-H.; Kim, K.-S.; and Lee, S. 2022. Inertial-Measurement-Unit-Based Novel Human Activity Recognition Algorithm Using Conformer. <u>IEEE Sensors</u>, 22(10): 3932.
- Klumpp, M.; Hesenius, M.; Meyer, O.; Ruiner, C.; and Gruhn, V. 2019. Production logistics and human-computer interaction—state-of-the-art, challenges and requirements for the future. The International Journal of Advanced Manufacturing Technology, 105(9): 3691–3709.
- Kong, Q.; Wu, Z.; Deng, Z.; Klinkigt, M.; Tong, B.; and Murakami, T. 2019. MMAct: A Large-Scale Dataset for Cross Modal Human Action Understanding. In <u>Proceedings of the IEEE International Conference on Computer Vision</u>.
- Kuehne, H.; Arslan, A.; and Serre, T. 2014. The language of actions: Recovering the syntax and semantics of goal-directed human activities. In <u>Proceedings of the IEEE Conference on Computer Vision and Pattern Recognition</u>, 780–787.
- Lago, P.; Takeda, S.; Adachi, K.; Alia, S. S.; Matsuki, M.; Benai, B.; Inoue, S.; and Charpillet, F. 2020. Cooking activity dataset with macro and micro activities.
- Loshchilov, I.; and Hutter, F. 2016. Sgdr: Stochastic gradient descent with warm restarts. <u>arXiv preprint</u> arXiv:1608.03983.

- Michel, R. 2016. 2016 warehouse/DC Operations Survey: Ready to confront complexity.
- Morales, J.; Yoshimura, N.; Xia, Q.; Wada, A.; Namioka, Y.; and Maekawa, T. 2022. Acceleration-based Human Activity Recognition of Packaging Tasks Using Motif-guided Attention Networks. In Proceedings of the IEEE International Conference on Pervasive Computing and Communications, 1–12. IEEE.
- Münzner, S.; Schmidt, P.; Reiss, A.; Hanselmann, M.; Stiefelhagen, R.; and Dürichen, R. 2017. CNN-based sensor fusion techniques for multimodal human activity recognition. In <u>Proceedings of the ACM International Symposium</u> on Wearable Computers, 158–165.
- Niemann, F.; Lüdtke, S.; Bartelt, C.; and Ten Hompel, M. 2022. Context-aware human activity recognition in industrial processes. Sensors, 22(1): 134.
- Niemann, F.; Reining, C.; Moya Rueda, F.; Nair, N. R.; Steffens, J. A.; Fink, G. A.; and Ten Hompel, M. 2020. LARa: Creating a Dataset for Human Activity Recognition in Logistics Using Semantic Attributes. <u>IEEE Sensors</u>, 20(15): 4083.
- Offi, F.; Chaudhry, R.; Kurillo, G.; Vidal, R.; and Bajcsy, R. 2013. Berkeley mhad: A comprehensive multimodal human action database. In <u>Proceedings of the IEEE Workshop on Applications of Computer Vision</u>, 53–60. IEEE.
- Reining, C.; Niemann, F.; Moya Rueda, F.; Fink, G. A.; and ten Hompel, M. 2019. Human activity recognition for production and logistics—a systematic literature review. Information, 10(8): 245.
- Schlögl, D.; and Zsifkovits, H. 2016. Manuelle Kommissioniersysteme und die Rolle des Menschen. <u>Berg</u> Huettenmaenn Monatsh, 161: 225–228.
- Sener, F.; Chatterjee, D.; Shelepov, D.; He, K.; Singhania, D.; Wang, R.; and Yao, A. 2022. Assembly101: A Large-Scale Multi-View Video Dataset for Understanding Procedural Activities. In <u>Proceedings of the IEEE/CVF Conference on Computer Vision and Pattern Recognition</u>, 21096–21106.
- Singh, S. P.; Sharma, M. K.; Lay-Ekuakille, A.; Gangwar, D.; and Gupta, S. 2020. Deep ConvLSTM with self-attention for human activity decoding using wearable sensors. IEEE Sensors, 21(6): 8575–8582.
- Spriggs, E. H.; De La Torre, F.; and Hebert, M. 2009. Temporal segmentation and activity classification from first-person sensing. In <u>Proceedings of the IEEE Computer Society Conference on Computer Vision and Pattern Recognition Workshops</u>, 17–24. IEEE.
- Stein, S.; and McKenna, S. J. 2013. Combining embedded accelerometers with computer vision for recognizing food preparation activities. In <u>Proceedings of the ACM International Joint Conference on Pervasive and Ubiquitous Computing</u>, 729–738.
- Xia, Q.; Korpela, J.; Namioka, Y.; and Maekawa, T. 2020. Robust Unsupervised Factory Activity Recognition with Body-worn Accelerometer Using Temporal Structure of Multiple Sensor Data Motifs. Proceedings of the ACM on

Interactive, Mobile, Wearable and Ubiquitous Technologies, 4(3): 1–30.

Xia, Q.; Wada, A.; Korpela, J.; Maekawa, T.; and Namioka, Y. 2019. Unsupervised factory activity recognition with wearable sensors using process instruction information. Proceedings of the ACM on Interactive, Mobile, Wearable and Ubiquitous Technologies, 3(2): 1–23.

Yan, S.; Xiong, X.; Arnab, A.; Lu, Z.; Zhang, M.; Sun, C.; and Schmid, C. 2022. Multiview transformers for video recognition. In Proceedings of the IEEE/CVF Conference on Computer Vision and Pattern Recognition, 3333–3343.

Yan, S.; Xiong, Y.; and Lin, D. 2018. Spatial temporal graph convolutional networks for skeleton-based action recognition. In Proceedings of the Thirty-second AAAI Conference on Artificial Intelligence.

Yavas, V.; and Ozkan-Ozen, Y. D. 2020. Logistics centers in the new industrial era: A proposed framework for logistics center 4.0. <u>Transportation Research Part E: Logistics and Transportation Review</u>, 135: 101864.

Yoshimura, N.; Maekawa, T.; Hara, T.; Wada, A.; and Namioka, Y. 2022. Acceleration-based Activity Recognition of Repetitive Works with Lightweight Ordered-work Segmentation Network. Proceedings of the ACM on Interactive, Mobile, Wearable and Ubiquitous Technologies, 6(2).

Zhang, Y.; Zhang, Z.; Zhang, Y.; Bao, J.; Zhang, Y.; and Deng, H. 2019. Human activity recognition based on motion sensor using u-net. IEEE Access, 7: 75213–75226.

7 Ethical Statement

This study is approved by the ethical committee of the institute of the authors.

8 Technical Appendix

8.1 OpenPack Dataset

Subjects Table 3 lists the metadata of the subjects and the number of recorded/annotated periods.

Modality The sensor data included in the dataset are summarized in Table 4. A total of 26 types of sensor data from 9 modalities (depth, keypoints, LiDAR, acceleration, gyroscope, quaternion, BVP, EDA, temperature) and readings from IoT devices are included. Fig. 7 shows the position of wearable sensors. Six sensors were attached to the participants' wrists and upper arms.

The metadata included in the dataset are summarized in Table 5. There are two types of metadata. Subject-related metadata include participants' experience with packaging tasks and annotations related to mistakes and accidents during the packaging works. Order-related metadata contains information that can be retrieved from an online order management system. These metadata are available at Open-Pack's website ⁴.

Activity Classes We annotated 10 types of work operations and 32 types of actions comprising work operations. The definitions of operation classes and action classes are listed in Table 6 and Table 7, respectively. The work operation classes were defined with reference to the work instructions. Action classes were selected mainly for those with clear movements to maintain high-quality annotation. In principle, each class was labeled by determining the start and end points. However, some activity classes were labeled with priority given to either the start or end point. In that case, the column "align" in Table 7 was labeled as "head" and "tail," respectively. Blank cells indicate that both the starting and ending points have been carefully checked.

Recording Scenarios The difficulties in packaging work recognition depend on various factors in logistics centers, which are described as follows. (i) Some logistics centers do not ask workers to strictly follow work instruction documents. Therefore, some experienced workers alter operational procedures slightly according to their personal preferences to improve efficiency. (ii) The variety of items to pack depends on orders. When a large item is included in an order, for example, the observed sensor data may differ from those of an order with normal items. (iii) Depending on the items to be packed and/or surrounding situations, a worker performs irregular actions or activities. (iv) Due to seasonal events or flash sales, task volumes for each worker may temporarily increase. In such case, workers' movement speed changes compared to an ordinary situation, resulting in noticeably different sensor data compared to the ordinary situation. Therefore, we have prepared the four scenarios to simulate these situations as follows.

 Scenario 1: In this scenario, we asked the subjects to follow the work instructions as much as possible. A list of items in an order was determined based on order sheets collected in actual logistics centers, and the probabilities

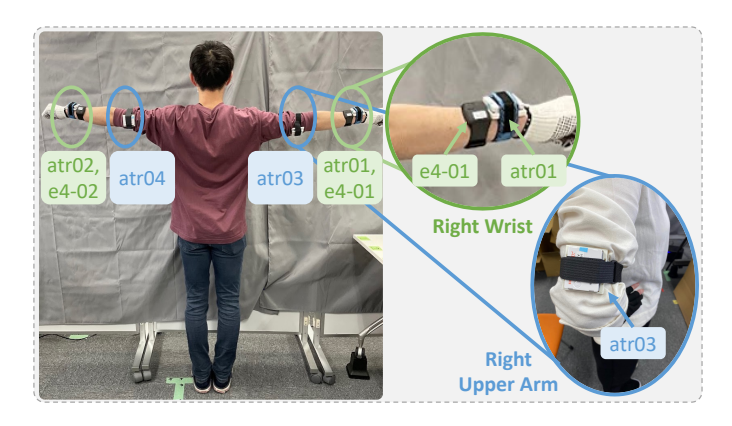


Figure 7: Wearable sensor position

with which very large or small items were included in an order were higher than the actual probabilities. In addition, the variety of items to be packed was limited (54 items). The number of items in an order was 1.83 on average.

- Scenario 2: In this scenario, we encouraged the subjects to alter the procedure of operations at their discretion. In addition, the probabilities with which quite large or small items were included in an order were lower than those of Scenario 1 (similar to actual probabilities), which made recognizing related operations with supervised learning difficult due to the data imbalance issue. The number of items in an order was 2.04 on average. In addition, we added 21 new items.
- Scenario 3: In this scenario, irregular situations/actions were added to Scenario 2. (i) Some shipping boxes were already assembled (because of mistakes, for example) and were available for workers to use. (ii) When small items (such as dry-cell batteries) were included in an order, a subject was also asked to put them in a paper bag. (iii) When multiple consecutive orders included only small items, a subject could bring them from the back table to the workbench at the same time.
- Scenario 4: To simulate a busy working time, we rushed the subjects by introducing an auditory alarm in Scenario 3. We measured the average duration of a work period performed by a subject in prior sessions, and we started periodic alarms (30-45 s interval) when the elapsed time of a period exceeded about 80% of the average duration.

⁴https://open-pack.github.io

Table 3: Overview of subjects. If the number of annotated periods differed from that of the recorded periods, the number of annotated periods are written in parentheses next to the number of recorded periods.

Subject			Dominant	Work Experience	# of	f recorded p	eriods [perio	ods]	
IĎ	Sex	Age	Hand	Experience			Scenario 3		Note
U0101	F	-	Right	-	100	0	0	0	
U0102	F	-	Right	-	94	0	0	0	
U0103	F	50s	Right	6 Months	100 (90)	0	0	0	
U0104	F	50s	Right	1 Month	70 (69)	0	0	0	
U0105	F	30s	Right	4 Years	100	0	0	0	
U0106	F	40s	Right	1 Month	90	0	0	0	
U0107	F	40s	Right	3 Years	100 (89)	0	0	0	
U0108	F	30s	Right	3 Years	100	0	0	0	
U0109	M	30s	Left	6 Months	100 (96)	0	0	0	
U0110	F	40s	Right	10 Months	100	0	0	0	
U0111	F	50s	Right	2 Years	100	0	0	0	
U0201	M	20s	Right	No Experience	0	40 (32)	40	20	
U0202	F	30s	Right	4 Years	0	40	40	14	Same subject as U0105
U0203	F	30s	Right	3 Years	0	40	40	20	Same subject as U0108
U0204	F	40s	Right	1 Year	0	40	40	20	Same subject as U0110
U0205	F	40s	Right	3 Years	0	40	40	20	Same subject as U0107
U0206	M	20s	Right	No Experience	0	40	40	20	
U0207	F	40s	Right	20 Months	0	40	40	20	
U0208	M	20s	Right	No Experience	0	40	40	20	
U0209	M	20s	Right	No Experience	0	40	40	20	
U0210	F	50s	Right	3 Months	0	40	40	20	Same subject as U0103

Table 4: Sensor data types in the OpenPack dataset

#	Category	Device	Sensor	Position	Product		
1 2	Vision	kinect	Depth Keypoints	Front View	Azure Kinect DK		
3	VISIOII	rs02	Depth	Top View	Intel® RealSense TM Depth Camera D435i		
4		LiDAR	Point Cloud	Front View	ULTRA PACK (VLP-32C) - Velodyne		
5		atr01	Acc Gyro	Right Wrist	ATR TSND151		
7		40.01	Quaternion	Tight Wilst			
8			Acc				
9		atr02	Gyro	Left Wrist	ATR TSND151		
10			Quaternion				
11			Acc		ATR TSND151		
12		atr03	Gyro	Right Upper Arm			
13			Quaternion				
14	Wearable		Acc				
15	vvcarable	atr04	Gyro	Left Upper Arm	ATR TSND151		
16			Quaternion				
17			Acc				
18		e4-1	BVP	Right Wrist	E4 wristband		
19		0.1	EDA	Tagit Wilst	21 Wilstould		
20			Temperature				
21			Acc				
22		e4-2	BVP	Left Wrist	E4 wristband		
23			EDA	2011 111111	2. Wilsteand		
24			Temperature				
25		ht	log	_	8001-C Portable Terminal		
	IoT Device	(,			CIPHER LAB - 8000 series Terminal		
26		label-printer	log	-	pseudo log data		

Table 5: Metadata in the OpenPack dataset

Category	Data	Description	Attributes
Subject-related	subject	participants' attributes	participants' experience in packaging tasks, their domi-
Subject-related			nant hand, gender, and age.
	irregular notes	manually annotated notes of the irregular activ-	category, time, description of the mistaks etc.
		ities such as mistakes.	
Order-related	item list	metadata about products used in the experiment	item_id, name, JAN code, size, size category, amount
Older-related	order list	a list of items to be packed in each box	order no, session no, box no, item combination pattern,
			item_id

Table 6: Definition of operation labels

ID	Name	Description					
100	Picking	Check the order-sheet and go to the back table to pick up the items.					
200	Relocate Item Label	peal off the label from the items and place it on the bottom margin of the order sheet. Check the item names and quantity on the list and label with a ballpoint pen.					
300	Assemble Box	Assemble cardboard boxes that match the size of the items.					
400	Insert Items	Put the goods into the box. Fill the box with an air cushion.					
500	Close Box	Close the box with craft tape.					
600	Attach the Box Label	Attach the box number label to the side of the box.					
700	Scan Label	Scan the barcodes with the handheld scanner in the following order: (1) order sheet, (2) box number sticker, (3) item label. Then, press the "ESC" button on the handheld scanner twice. Next, scan the barcodes with the scanner of the label printer in the following order: (1) order sheet, (2) code on the label printer.					
800	Attach Shipping Label	Attach the shipping label printed out by the label printer to the box.					
900	Put on Back Table	Move the completed packing box under the back table.					
1000	Fill out Order Sheet	Sign the confirmation column of the order sheet and insert it into the tray of completed order sheets.					
8100	Null						

Table 7: Definition of the action labels

Operation	ID	Action	Description	Alignment
	101	Pick Up Sheet	Pick up the order sheet from the workbench.	
D: -1-:	103	Pick Up Item From Box	Pick items out of the box that contains items picked in batches.	
Picking	107	Pick Up Box Sheet	Pick up an order sheet and packed boxes simultaneously. (This	
		-	label is used for moving packed boxes and picking items for the	
			next box simultaneously.)	
	108	Walk to Work Bench	Lift the item and turn back toward the workbench. (When pick-	
			ing is performed in one round trip, this action is set as the be-	
			ginning of the box.)	
	109	Put Packed Box	Go to the back table and place the packed box under the table.	
	201	Remove the Item Label	Remove the sticker with the barcode from each item.	
	204	Write Check Mark	The subject's hand touches the pen.	
Relocate Item Label	205	Put Item Small Bag	Put small items into a small paper bag.	
	301	Pick Cardboard	Select and pick up the boxes that match the size of the items.	
	302	Bend Flap	Bend the four flaps of the box.	
Assemble Box	303	Attach Tape	Apply craft tape to close the bottom of the box.	
	304	Turn Over Box	Turn the box upside down so that the side with the craft tape is	
			on the bottom.	
	305	Pick Up Assembled Box	Pick up a pre-assembled box. (Used in Scenarios 3-5)	
	401	Insert Item into Box		
[]4	403	Separate Air Cushion	Tear off the connected cushioning.	tail
Insert Items	404	Put Item in a Small Bag	Insert small the items (<10cm) into the small paper bag and	
			close it with tape.	
Cl D	501	Bend Flap	Bend four flaps in the upper side of the box.	
Close Box	502	Attach Tape	Close the box with a craft tape.	
Λ.μ l. D I - l l	601	Attach Box Label	Place the box number label on the side of the box.	
Attach Box Label	701	Pick Up HT	Pick up handheld scanner (HT).	head
	702		Scan the order ID code in the upper-left corner of the order	tail
			sheet.	
Scan Label	703	Scan Box	Scan the box number label.	tail
	704	Scan Item	Scan each item number on the label on the order sheet individ-	tail
			ually.	
	706	Scan Order Sheet	Scan the order ID code in the upper-left corner of the order sheet	tail
			with the white scanner.	
	707	Scan Printer	Scan the code on the label printer to print out the shipping la-	tail
			bels.	
A., 1 (1) 1 1 1 1	801	Pick Up Shipping Label	Pick up the shipping label from the label printer.	
Attach Shipping Label	802	Attach Shipping Label	Attach the printed shipping label to the upper side of the box.	
D (O D 1 TIII		Pick Up Packed Box	Pick up prepared box from the workbench.	head
Put On Back Table		Put Packed Box	Go to the back table and place the packed box under the table.	tail
		Pick Up Pen	The subject's hand touches the pen.	head
Fill out Order		Write Sign	Sign each field in the column next to the item list on the order	
			sheet.	
	1002	Push Order Sheet Into Tray	Insert order sheet into the tray for the completed order sheets.	

8.2 Implementation Details of LTS-Net

We implemented two types of LTS-Net; *LTS-Net* (*WPCP*) and *LTS-Net* (*Conformer*) which use a WPCP module (Yoshimura et al. 2022) or a conformer block as the feature extractor. Here, we describe the implementation details of these models. Note that we used the score of *LTS-Net* (*WPCP*) in the main document because the performance was somewhat higher than *LTS-Net* (*Conformer*).

Encoder The encoder performs initial feature extraction and downsampling from the raw sensor data. It comprises four convolution layers, and GELU is used as the activation function. The kernel and filter sizes (embedding dimension for the feature extractor) are 31 and $Ch_{en}=128$, respectively. The stride of the second and fourth convolution layers is set to 2 for downsampling. The stride of the other layers is 1. Anchor \boldsymbol{a} is also downsampled into the same sampling rate as the output of the fourth convolution, i.e., 7.5 Hz. A pseudo-label $\hat{\boldsymbol{y}}_0$ and an anchor mask M_A are initialized using this downsampled anchor.

Feature Extractor - LTS-Net (WPCP) Figure 8 shows the architecture of the feature extractor used in *LTS-Net (WPCP)*. We used the WPCP module proposed by Yoshimura et al. (Yoshimura et al. 2022). We used the same architecture as the original model except for the kernel size and dilation rate. In the original model, the input sensor data sequence was downsampled to 1/8 in the encoder. In contrast, in LTS-Net, the input sensor data sequence was downsampled to 1/4 in the encoder. Therefore, the kernel size and dilation rates were expanded to retain the large receptive field. The embedding dimension Ch_{em} of x_l is set to 128 for the all blocks.

Feature Extractor - LTS-Net (Conformer) The feature extractor of this model is the conformer block (Kim et al. 2022). The kernel size for the convolution layer, # of the MHSA (Multi-Head Self-Attention layer) heads, and embedding dimension Ch_{em} are set to 31, 4, and 128, respectively.

Bidirectional Feedback Block The BF block consists of a feature extractor and two feedback branches. In the feedback branch from the anchor stream to the feature stream, smoothing is performed on the pseudo-label $\mathbf{\acute{y}}_{l-1}$. First, a copy of $\mathbf{\acute{y}}_{l-1}$ is created and smoothed by computing a moving average with the window size 17 and 21 for the model using Conformer and WPCP as the feature extractor respectively. We denote this smoothed pseudo-label as $\mathbf{\acute{y}}_{l-1}^{sm}$. To preserve the anchor value, we update the pseudo-label $\mathbf{\acute{y}}_{l-1}$ using the anchor mask with the following formula:

$$\mathbf{\acute{y}}_{l-1} \leftarrow (1 - M_A)\mathbf{\acute{y}}_{l-1} + M_A\mathbf{\acute{y}}_{l-1}^{sm}.$$

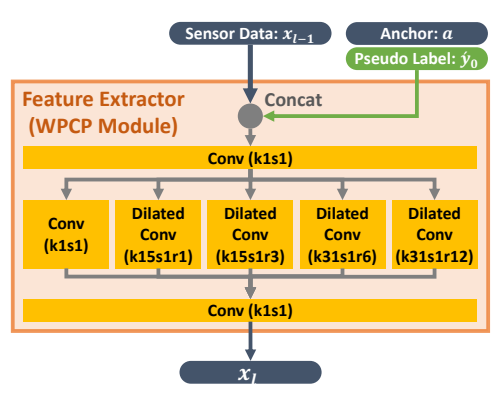


Figure 8: WPCP Module. "k15s1r3" represent the parameters of the convolution layer, indicating that kernel size (k) is 15, stride (s) is 1, and dilation rate (r) is 3.

The feature extractor takes x_{l-1} and y_{l-1} as input features and outputs a tensor with the same shape as x_{l-1} . The details of the feature extractor are described above.

In the feedback branch from the feature stream to the anchor stream, the output of the feature extractor $\boldsymbol{x}_l \in \mathbb{R}^{Ch_{em} \times T}$ is transformed into the same shape as the $\boldsymbol{\mathring{y}}_{l-1}$ and used to calculate $\boldsymbol{\tilde{y}}_l \in \mathbb{R}^{N_C \times T}$. This transformation is performed by a single pointwise convolution followed by a sigmoid function. The blending of $\boldsymbol{\mathring{y}}_{l-1}$ and $\boldsymbol{\tilde{y}}_l$ is performed using the following formula:

$$\mathbf{\acute{y}}_{l} = (1 - \beta M_{A})\mathbf{\acute{y}}_{l-1} + \beta M_{A}\mathbf{\~{y}}_{l}.$$

In the experiment, β is set to 0.25.

The number of BF blocks is one of the important hyperparameters in LTS-Net. In our experiment, the number of BF blocks was set to 16 and 8 for *LTS-Net* (*WPCP*) and *LTS-Net* (*Conformer*), respectively.

Output Layer of the Feature Stream To acquire the output from the feature stream \hat{y}_{out} , pointwise convolution is applied to the output of the feature extractor in the last BF block. As the output from the anchor stream, which is the final output of LTS-Net, the output from the last BF block is directly used.

Initialization of the Inputs of the Anchor Stream We introduced $C(\boldsymbol{a},t)$ as a function that returns the possible activity classes at time t. By analyzing the training data, we obtained a list of correspondences between IoT devices and activity classes. For example, when we focused on an IoT device, we retrieved a set of activity classes that occurred when the device was used in the training data. The activity classes are the possible activity classes when the IoT device is used. Based on the set of activity classes, $C(\boldsymbol{a},t)$ determines the possible activity classes at time t. $C(\boldsymbol{a},t)$ checks the anchor data \boldsymbol{a} at time t to determine whether an IoT device was used. If an IoT device was used, it returns the set of activity classes associated with the IoT device as the possible activity classes.

Loss of LTS-Net The loss of LTS-Net is a sum of two softmax cross-entropy loss functions, as formulated in the main

Table 8: Train, validation, and test split

Split	Subject	Session	Note
Train	U0101	S0100, S0200, S0300, S0400, S0500	
	U0102	S0100, S0200, S0300, S0400, S0500	
	U0103	S0100, S0200, S0300, S0400, S0500	
	U0105	S0100, S0200, S0300, S0400, S0500	
	U0106	S0100, S0200, S0300, S0400, S0500	
	U0107	S0100, S0200, S0300, S0400, S0500	
	U0109	S0100, S0200, S0300, S0400, S0500	
	U0110	S0100, S0200, S0300, S0400, S0500	
Validation	U0111	S0100, S0200, S0300, S0400, S0500	
Test	U0104	S0100, S0300, S0400	Beginner
	U0108	S0100, S0200, S0300, S0500	Medium
	U0110	S0100, S0200, S0300, S0400, S0500	Expert

text. The hyperparameter γ , which controls the impact of \hat{y}_{out} , was set to 0.1 in this experiment.

8.3 Evaluation Details

Training/Testing Split Table 8 shows the data used for the training, validation, and testing in the evaluation section. The test data comprise three subjects with skill levels of beginner, medium, and expert determined by the experimenter. Note that the participant U0109 was included in the training data, but was not used in the experimental training process because he was the only left-handed subject in the dataset.

Acceleration data from the left wrist were used as the only input to the model because the experiment assumed a smartwatch was worn on the non-dominant hand to collect data.

Details of Comparative Methods In principle, the parameters of the comparative methods were identical to those in the original studies. However, some parameters were not fixed, such as kernel size and the number of layers. These parameters were tuned to fit the OpenPack dataset. The parameters used in the experiments for each method were as follows.

- **DCL-SA:** The Tensorflow implementation is provided by the authors of the original paper (Singh et al. 2020)⁵. We converted the code for PyTorch. The parameters of the model used in the experiments were as follows: # convolution layers = 1, # convolution filters = 64, # LSTM layers = 1, # LSTM units = 128, # MHSA (Multi-Head Self-Attention layer) heads = 8.
- **DCL-SA** (**Early**): This is an early fusion version of *DCL-SA*. Data from IoT devices were resampled and concatenated to acceleration data first and fed to the model. Therefore, the dimension of the input sequence is 5 (Acc 3ch + IoT 2ch).
- **DCL-SA** (**Late**): This is a late fusion version of *DCL-SA*. Acceleration data and data of IoT devices are encoded in the different convolution layers. The encoded features are concatenated before MHSA.
- Conformer: The implementation of conformer blocks

- is based on the model released in the Torchaudio⁶. The model design and parameters were based on the paper by Kim et al. (Kim et al. 2022) and tuned to the OpenPack dataset. The parameters used in this experiment were as follows: latent sequence embedding dimension = 128, # MHSA head = 4, kernel size for convolution layers = 31. In the conformer block, a convolution module was applied after an attention module.
- **Conformer** (**Early**): This is an early fusion version of *Conformer*. Data from IoT devices were resampled and concatenated to acceleration data and then fed into the model. Therefore, the dimensionality of the input sequence was 5.
- LOS-Net: This model was designed for and evaluated on the activity recognition of the packaging work. Parameters defined in the study (Yoshimura et al. 2022) were used. LOS-Net requires a graph describing a workflow as additional information. For a fair comparison, we used LOS-Net(-R), which does not use the graph.
- **LOS-Net** (**Early**): This is an early fusion version of *LOS-Net*. Data from IoT devices were resampled and concatenated to acceleration data and then fed into the model. Therefore, the dimensionality of the input sequence was 5 (Acc 3ch + IoT 2ch).
- LOS-Net (Late): This is a late fusion version of LOS-Net. Features extracted from acceleration data and data from IoT devices were concatenated directly after the LOS-Net's encoder and the fused feature was fed into the decoder of the LOS-Net.

In the above methods, value clipping with -3G/+3G as the lower/upper bounds and normalization were performed as preprocessing. Thus, the range of input values was [0,1]. Sliding windows were also applied. The window size N_T was set to 60 s (= 1800 pt) according to (Yoshimura et al. 2022). In addition, during training, a random crop was applied, extracting a window from a random position to prevent overfitting.

Evaluation Metrics Because the OpenPack dataset suffers from the class imbalance problem, i.e., the number of samples for each class is highly variable, we used the macro average of F1-measure as a robust metrics to this problem. When we calculate the metric, we first downsampled the model's output, i.e., series of activity class IDs, to 1 Hz, which is the sampling rate of the ground truth, to compute the F1-measure for each class. Then, the macro average of F1-measure is calculated by averaging the F1-measures over all the classes, which is a robust metric against the class imbalance problem. In addition, we computed the weighted average of the F1-measure, which is calculated by taking the weighted average of the number of samples in each activity class. This metric is more sensitive to the class imbalance problem.

Hyperparameters for Optimization We performed a grid search to find better hyperparameters for each model.

⁵https://github.com/isukrit/encodingHumanActivity

⁶https://pytorch.org/audio/main/_modules/torchaudio/models/conformer.html

The hyperparameters tuned included the type of optimizer (two types), learning rate scheduler (three types), and initial values of learning rate (five types). For the optimizer, the choices were SGD as used in paper on LOS-Net, and Adam used in the works on DCL-SA and Conformer. For the learning rate scheduler, three methods are available: a method that does not use scheduler (None), a method that decays the learning rate by applying $\gamma = 0.9$ every five epochs (StepLR), and a cosine annealing scheduler ($Cosine\ Annealing$) (Loshchilov and Hutter 2016). The initial value of the learning rate is selected from $lr = \{5.0 \times 10^{-2}, 10^{-3}, 10^{-3}, 10^{-4}\}$.

For each setting, models were trained for 300 epochs and tested using the model with the lowest validation loss. To improve the reliability of the results, we repeated the same experiment for 5 times with different random seeds and selected the best hyperparameter settings with the highest average F1-measure over 5 runs. The hyperparameters selected for each method and the model performance with standard deviation are shown in Table 9, indicating the stable performance of LTS-Net. For most of the methods, the Adam optimizer without a learning rate scheduler was selected.

Hardware Settings We used a GPU cluster to manage our experiment. The GPU cluster consists of nine nodes with 2–4 GPUs. The GPUs used in the experiments were *Geforce GTX 1080* (memory: 8GB), *GeForce RTX 2070* (8GB), *Titan RTX* (24GB), *GeForce RTX 3090* (24GB), and *Quadro RTX 8000* (48GB). The Conformer model was trained on GPUs with memory size ≥ 24 GB due to the large memory consumption. The other models were assigned to available GPUs.

Ablation Study Ablation study was conducted to investigate the effectiveness of the modules in LTS-Net. We prepared the following methods. Each method was implemented based on both *LTS-Net (WPCP)* and *LTS-Net (Conformer)*.

- w/o Anchor: This model does not use data from IoT devices. The anchor a is replaced with a dummy anchor tensor, whose shape is the same as a and all the elements are initialized as 0.
- Early Fusion: The early fusion model of LTS-Net. The data from IoT devices are fed into the sensor stream as like the other early fusion model. The dummy anchor tensor is used as an input to the anchor stream.

Table 10 shows the results of the ablation study. The use of anchor (data from IoT devices) has the greatest impact on the recognition accuracy, decreasing the score by up to 0.045 in the F1-measure (macro; All) when anchor is not available. The F1-measure of U0104 does not differ significantly among the methods. This may be because the skill level of U0104 was beginner and the speed of movements were relatively slow and easier to recognize. As for the sensor fusion strategy, the score of the *Two-stream* approach, which is used in the proposed LTS-Net, tended to improve the score by about 0.02 compared to the early fusion models.

8.4 Information on Related Dataset

The datasets of the related studies are summarized in Table 1 in the main text. The attributes in the table were primarily collected from the original papers or those compiled in their related papers. However, because some attributes are not described in the papers, we calculated these attribute values by ourselves. Here, we explain the procedure to compute the missing values.

UTD-MHAD The recording length was not described in the original paper. We downloaded the dataset and counted the number of records in the IMU data. We found 26,880 records in total. Because the sampling rate of the acceleration data was 50 Hz, we estimated the recording length to be 9 min.

MMAct The *recording length* was not described in the original paper. The smartphone's acceleration data (*sensor/acc_phone_clip*) contained 6,331,335 data samples in total. Because the sampling rate of the acceleration data was 100 Hz, we estimated the recording length as 17 h and 35 min

50 Salads The # of annotated instances (# of activity instances) was unavailable in the original paper. We downloaded the dataset and counted the number of records in text files under ann-ts/activityAnnotations, resulting in 2,967 records from 54 text files.

IKEA-ASM The # of annotated instances (# of activity instances) was unavailable. We downloaded the dataset and counted the number of records in text files under action_annotations/gt_segments.json, resulting in 8,413 annotated instances.

Assembly101 The original paper (Sener et al. 2022) only lists the total recording footage, which was 513 h. We divided this value by the number of views, 12, to obtain the *recording length*.

InHARD The number of frames is mentioned in the paper, but the *recording length* and # of annotated instances were not given. In the paper, the authors described that the number of frames was more than 2M and the framerate of RGB video was 30 fps. Based on this information, we estimated the recording length to be approximately 2,000,000 frames /(30 fps $\times 3600) = 18.5$ h. As for the # of annotated instances, while the uploaded dataset was corrupted, which made it impossible to access this information, the description on the data download site described that the dataset contained 4800 action samples. Therefore, we used this number.

ABC Bento The # of work periods, # of annotated instances, and recording length were not described. As for the # of work periods and annotated instances, we downloaded the dataset and counted them. The recording length was estimated as 3 h and 22 min by dividing the total number of data points (1,213,760 points) in the dataset by the sampling rate of 100 Hz.

⁷https://zenodo.org/record/4003541#.YvNPp-zP28c

Table 9: Hyperparameters selected through grid search

	Selected Parameters			Macro	Avg.	Weighted Avg.	
Model	Optimizer	Scheduler	lr	mean	(std)	mean	(std)
DCL-SA	SGD	None	5.0×10^{-2}	0.752	0.015	0.766	0.015
DCL-SA (Early)	Adam	None	10^{-3}	0.760	0.013	0.780	0.012
DCL-SA (Late)	Adam	None	10^{-3}	0.797	0.021	0.813	0.020
Conformer	Adam	None	10^{-3}	0.748	0.022	0.752	0.023
Conformer (Early)	Adam	None	10^{-3}	0.787	0.026	0.797	0.024
LOS-Net	Adam	None	10^{-3}	0.755	0.019	0.762	0.010
LOS-Net (Early)	Adam	None	10^{-4}	0.784	0.011	0.802	0.010
LOS-Net (Late)	Adam	None	10^{-4}	0.777	0.011	0.787	0.013
LTS-Net (Conformer)	SGD	None	5.0×10^{-2}	0.818	0.005	0.832	0.003
LTS-Net (WPCP)	Adam	Cosine Annealing	10^{-4}	0.830	0.009	0.846	0.008

Table 10: Results of the ablation study.

	Anchor*	F1 (Macro Avg.)				F1 (Weighted Avg.)	
Base Model	(IoT Device)	Fusion	U0104	U0108	U0110	All	All
	√	Two Stream	0.847	0.815	0.752	0.818	0.832
LTS-Net (Conformer)	✓	Early Fusion	0.854	0.790	0.739	0.803	0.816
	-	-	0.847	0.719	0.709	0.773	0.781
	√	Two Stream	0.847	0.842	0.757	0.830	0.846
LTS-Net (WPCP)	✓	Early Fusion	0.849	0.809	0.730	0.807	0.822
	-	-	0.843	0.777	0.676	0.778	0.791

^{*} A check mark (\checkmark) denotes that the input includes anchor (data from IoT devices).

LARa # of annotated instances was not described in the original paper. In LARa, a label was assigned to each acceleration data sample (data point). Therefore, # of annotated instances was calculated from the annotations assigned to the acceleration data, combining consecutive labels with the same class as a single instance. Because the acceleration data of the picking work was missing for some subjects, # of annotated instances for only the packaging work (Scenario 3) was counted, and 1,526 instances were found.